

Virginia Commonwealth University
VCU Scholars Compass

Physics Publications

Dept. of Physics

2003

H-substituted anionic carbon clusters C_nH^- ($n \leq 10$): Density functional studies and experimental observations

L. Pan

Virginia Commonwealth University

B. K. Rao

Virginia Commonwealth University

A. K. Gupta

Bhabha Atomic Research Centre

G. P. Das

Bhabha Atomic Research Centre

P. Ayyub

*Tata Institute of Fundamental Research*Follow this and additional works at: http://scholarscompass.vcu.edu/phys_pubs Part of the [Physics Commons](#)

Pan, L., Rao, B. K., Gupta, A. K., et al. H-substituted anionic carbon clusters C_nH^- ($n \leq 10$): Density functional studies and experimental observations. *The Journal of Chemical Physics* 119, 7705 (2003). Copyright © 2003 AIP Publishing LLC.

Downloaded from

http://scholarscompass.vcu.edu/phys_pubs/169

This Article is brought to you for free and open access by the Dept. of Physics at VCU Scholars Compass. It has been accepted for inclusion in Physics Publications by an authorized administrator of VCU Scholars Compass. For more information, please contact libcompass@vcu.edu.

H-substituted anionic carbon clusters C_nH^- ($n \leq 10$): Density functional studies and experimental observations

L. Pan^{a)} and B. K. Rao

Department of Physics, Virginia Commonwealth University, Richmond, Virginia 23284-2000

A. K. Gupta

Nuclear Physics Division, Bhabha Atomic Research Centre, Mumbai 400085, India

G. P. Das

TPPED, Physics Group, Bhabha Atomic Research Centre, Mumbai 400085, India

P. Ayyub

Department of Condensed Matter Physics, Tata Institute of Fundamental Research, Homi Bhabha Road, Mumbai 400005, India

(Received 1 April 2003; accepted 23 July 2003)

We have studied the interaction of hydrogen with small neutral and anionic carbon clusters using density functional calculations. The geometry, stability, and electronic structure of these clusters show an odd–even alternation originating in the bonding nature of the carbon atoms. Our mass spectrometric measurements of the abundance of C_nH^- ($n \leq 10$) cluster anions produced by gas-feed Cs sputtering from different crystallographic forms of carbon display similar odd–even alternation with the even- n clusters being relatively more abundant. The calculated trend in the adiabatic electron affinities shows a behavior similar to the experimental abundance pattern. We discuss a possible partial suppression of the chain-to-ring transformation (which normally occurs at $n=10$ in C_n^-) in C_nH^- and compare it with our density functional calculations as well as observations in C_nN^- . We also observe that the size dependence of the abundance of C_nH^- clusters sputter ejected from a fullerene target exhibits a distinctly different power-law decline compared to crystalline and amorphous carbon. © 2003 American Institute of Physics.

[DOI: 10.1063/1.1609400]

I. INTRODUCTION

The possibility of designing novel materials¹ by taking advantage of the size-dependent properties² of atomic clusters has created tremendous interest among both experimentalists and theoreticians, and has led to the study of various types of atomic clusters. Studies of small carbon clusters are of special interest due to their importance in combustion and pyrolysis, in astrophysical processes, and in the formation and growth of fullerenes³ and nanotubes,⁴ which are made up of five- and six-membered carbon rings. Some earlier studies on small carbon clusters^{5,6} have indicated that odd-numbered clusters prefer linear structures to ring structures. It is therefore not clear why the five-membered rings show up in fullerenes. Would a linear chain bend when attached to a six-atom ring? Can the isomers with linear chain and planar ring configurations coexist under normal experimental conditions? Are the “tadpole” structures very close in energy to the ground states? Such questions have prompted studies of both neutral and anionic carbon clusters.⁷ The study of anionic clusters is particularly interesting since photoelectron spectroscopy provides indirect information⁸ on their structure. Such theoretical investigations depend upon accurate experiments to verify their predictions. Earlier workers have

studied the reactivity of charged carbon clusters with gas molecules such as H_2 , D_2 , O_2 , CH_4 , C_2H_2 , C_2H_4 , CO , C_2N_2 , and HCN .⁹ To understand the role of substituents such as N on the electronic structure and stability of carbon clusters, C_nN^- clusters ($n \leq 10$) have been produced and their properties compared with those of C_n^- clusters.¹⁰ In this paper we study the hydrogenation of carbon clusters to see how the hydrogen atom explores the active site on a carbon cluster and thereby reveals its intrinsic structure.

H-substituted carbon clusters have gained importance following the discovery of long-chain carbon molecules in interstellar and circumstellar environments. These have been studied using various experimental techniques, including cluster vaporization source¹¹ and highly charged ion impact on solid C_{84} .¹² These studies show that the C_nH^+ ($n \leq 10$) cluster cations to be more abundant for odd n . H-substituted carbon cluster anions have earlier been generated using secondary-ion-mass spectrometry (SIMS),¹³ by irradiation of alkanes and benzene by ^{252}Cf fission fragments,¹⁴ and laser ablation.¹⁵ We have utilized the well-established gas-feed Cs-sputter technique, which has several advantages over SIMS and laser ablation. Generally, $^{12}C_nH^-$ cannot be distinguished from $^{12}C_{n-1}^{13}C^-$ (the natural abundance of ^{13}C is 1.108%), and there could also be ion signals with the same m/q due to residual impurities. In the case of the gas-feed sputter technique, these can be readily taken care of by subtracting the background signal (without gas spray) from the

^{a)}Current address: Department of Materials Science and Engineering, University of Pennsylvania, Philadelphia, PA 19104.

data. Here we report the results of our experimental measurements on C_nH^- in conjunction with *density functional* cluster calculations performed on pure C_n and C_n^- clusters as well as hydrogenated neutral and anionic carbon clusters. Both our calculations and experimental measurements indicate the presence of odd–even alternations in the geometry, stability, and electronic structure of the C_nH^- clusters. Such studies are expected to elucidate the microscopic mechanism of the interaction of hydrogen with small carbon clusters as a function of cluster size.

The paper is organized as follows. In Sec. II we present a density functional approach to understand the ground-state geometry, stability, and electronic structure of pure as well as hydrogenated carbon clusters, both neutral and anionic. Section III is devoted to a brief experimental overview of the production of monohydrogen-terminated carbon cluster anions from different crystallographic forms of carbon via the gas-feed Cs-sputter technique. This is followed by the results on C_nH^- yield as a function of cluster size and its interpretation in terms of their power-law behavior. We also discuss the effect of monohydrogen substitution of the carbon clusters on the chain to ring transformation that normally occurs at $n=10$. In Sec. IV we give a summary comparison of the theoretical and experimental results.

II. THEORETICAL STUDY OF PURE AND HYDROGENATED CARBON CLUSTERS

A. Method of calculation

We used the self-consistent-field linear combination of atomic orbitals-molecular orbitals (SCF-LCAO-MO) method to obtain the total energies of the clusters. The atomic wave functions were represented by an all-electron triple- ζ basis set with extra polarization functions (6-311G**).¹⁶ The total energies were calculated using the density functional theory (DFT) and generalized gradient approximation (GGA) for the exchange-correlation contribution. The Lee–Yang–Parr form of the correlation functional¹⁷ and the Becke exchange¹⁸ (B3LYP) were used with the GAUSSIAN 98 computational code¹⁶ for our calculations. The geometries were optimized for different spin multiplicities without any symmetry constraint. The optimization was performed for each cluster by starting with several initial structures to locate the geometry corresponding to the global minimum through an exploration of the potential energy surface.

B. Neutral carbon clusters

The energetics and equilibrium structures of the C_n clusters were studied up to $n=10$. The calculated equilibrium geometries are shown in Fig. 1 and the corresponding multiplicities and energies are given in Table I. The calculated bond length of C_2 , 1.317 Å, compares very well with values obtained from other methods,^{5,19} while the corresponding experimental value²⁰ is 1.312 Å. The theoretical binding energy per atom is 3.25 eV, while the experimental binding energy per atom²¹ is 3.04–3.15 eV. The calculated geometry for C_3 matches very well with other theories^{5,22} and experiment.²³ Our binding energy/atom of 4.75 eV is comparable to these earlier theoretical results as well as the experimental value^{5,7}

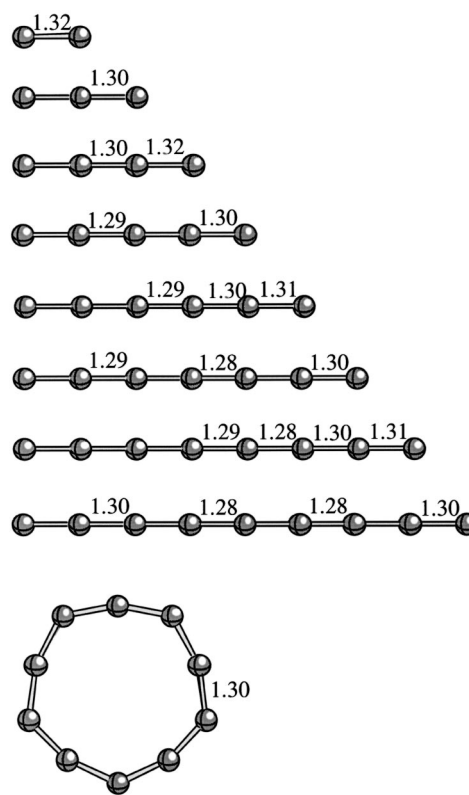


FIG. 1. Optimized ground-state geometries of the C_n ($n \leq 10$) clusters. The representative bond lengths are given in Å.

of 4.63 ± 0.2 eV. The geometries of C_n ($n=4-9$) are all linear and the bond lengths are very close to other theoretical values.^{24–29} The binding energies/atom for C_n ($n=4-9$) are 4.94, 5.46, 5.50, 5.75, 5.77, and 5.91 eV, respectively. These match very well with corresponding values of 4.65–4.95, 5.22–5.42, 5.33, 5.67, 5.53, and 5.92 eV, respectively, from various theories and experiments.^{5,7} The multiplicities presented in Table I have been verified against other theories⁵ and experiments⁷ when available and they match completely.

All the structures obtained by us are linear up to nine atoms, as also predicted by others. However, the ten-atom cluster is cyclic, as predicted by Raghavachari and Binkley.⁵ The binding energy/atom is 6.13 eV. The binding energy/atom increases steadily with minor odd–even oscillations, as usually observed for all types of small clusters.³⁰

C. Anionic carbon clusters

The ground-state geometries of C_n^- ($n=2-10$) clusters are shown in Fig. 2. Again, all geometries are linear up to $n=9$ and the ground state is cyclic for $n=10$. These geometries as well as the corresponding multiplicities reported in Table I match very well with the theoretical values of Raghavachari,²² Adamowicz,^{24,31} Ray and Rao,³² Watts *et al.*,²⁴ and the experimental values of Gotts *et al.*³³ The binding energies/atom obtained for these clusters ($n=2-10$) are 4.47, 5.15, 5.66, 5.86, 6.03, 6.10, 6.18, 6.22, and 6.21 eV, respectively, which match with the theoretical results of Raghavachari²² and Ray and Rao.³²

Table I also presents the electron affinities obtained in the current calculations and compares them with experimen-

TABLE I. Results from C_n and C_n^- calculations. ΔE indicates the energy released when an extra carbon atom is added to a preexisting cluster.

n	C_n			C_n^-			EA (eV)	
	Multiplicity	E (hartree)	ΔE (eV)	Multiplicity	E (hartree)	ΔE (eV)	Theory	Expt. ^a
1	3	-37.84267		4	-37.85634		0.37	
2	3	-75.92431	6.50	2	-76.02745	8.93	2.81	3.30
3	1	-114.05231	7.76	2	-114.11020	6.53	1.57	1.95
4	3	-152.09671	5.49	2	-152.21670	7.18	3.26	3.70
5	1	-190.21651	7.54	2	-190.30340	6.64	2.36	2.80
6	3	-228.26875	5.70	2	-228.39870	6.87	3.53	4.10
7	1	-266.37851	7.26	2	-266.48250	6.56	2.83	3.10
8	3	-304.43685	5.87	2	-304.57350	6.75	3.72	4.42
9	1	-342.54100	7.11	2	-342.65640	6.53	3.14	3.70
10	1	-380.67868	8.02	2	-380.72350	6.11	1.22	2.30

^aReference 6.

tal values. Note that our results are adiabatic electron affinities, which are the differences in the total energies of the ground-state anions and the corresponding ground-state neutral clusters. The experimental values are from the work of Yang *et al.*⁶ who have reported vertical electron detachment energies. These energies are obtained as the differences between the total energies of the ground-state anions and the corresponding neutral clusters in the same geometry as those of the anions. Because the neutral clusters are not relaxed, the vertical electron affinities (VEAs) are always higher than the adiabatic electron affinities (AEAs). Table I shows that the experimental values of the VEAs are consistently higher than the theoretical AEA values. The differences are of the order of 0.5 eV, which is typically the amount of energy

gained by relaxation to the final ground state of the neutral clusters. Note that our AEA values show an odd-even alternation and the behavior of the VEA values from experiment is very similar. A further discussion of these odd-even alternations follows later.

One can study the relative stabilities of clusters by calculating the incremental energy $\Delta E_n = E_{n-1} + E_1 - E_n$, where E_n corresponds to the total energy of a neutral or anion cluster containing n atoms and E_1 is the energy of a single carbon atom. Thus ΔE is the energy gained by forming an n -atom cluster through the addition of an extra carbon atom. The values of ΔE for C_n and C_n^- clusters (Fig. 3) show an interesting odd-even alternation. The peaks in ΔE occur for even n in the case of the anionic clusters, while it occurs for odd n in neutral clusters. A similar behavior is noticed for AEAs with the peaks occurring for even values of n . This is easily explained by the fact that a higher ΔE is indicative of a relatively higher stability for that particular cluster. Similarly, if a cluster has relatively higher electron affinity, the corresponding anion is comparatively more stable. For example, C_4 has higher AEA than C_3 or C_5 . This indicates that C_4^- is more stable than C_3^- or C_5^- , leading to a higher ΔE for C_4^- relative to C_3^- and C_5^- . This is exactly

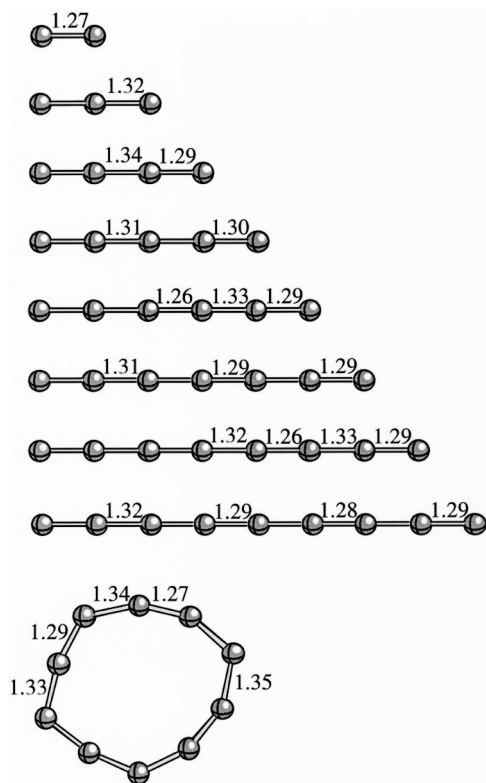


FIG. 2. Optimized ground-state geometries of the C_n^- ($n \leq 10$) clusters (bond lengths are in Å).

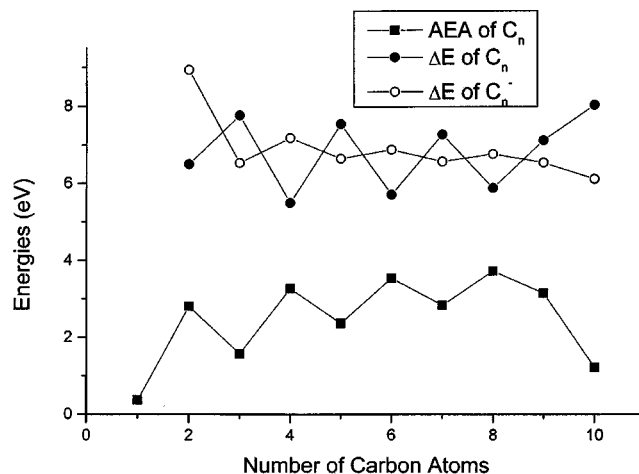


FIG. 3. Energy gain ΔE on addition of an extra C atom to C_n ($n \leq 10$) clusters (solid circles) and C_n^- clusters (open circles). The plots of adiabatic electron affinity of C_n clusters are shown by solid squares.

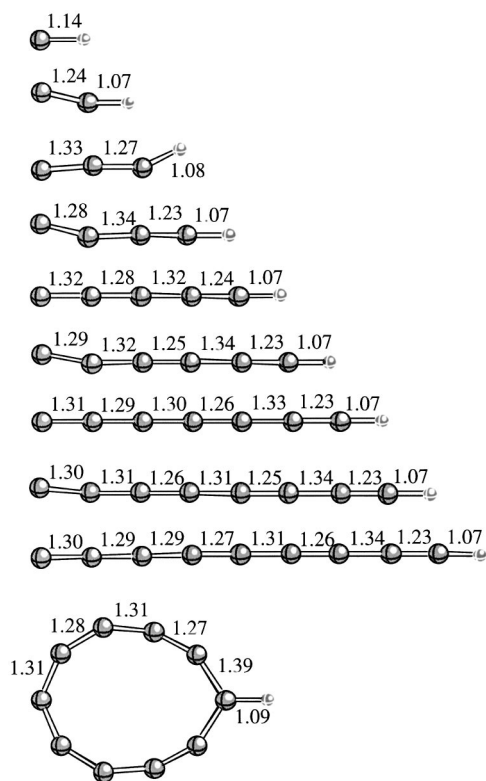


FIG. 4. Optimized ground state geometries of C_nH ($n \leq 10$) clusters (bond lengths are in Å).

what is observed in Fig. 3. While the anions are all spin doublets, the neutral cluster multiplicities oscillate between 1 and 3 for $n=2-9$ with the odd- n clusters being singlets. The reason for this lies in the electronic structures of the clusters and is related to the occupation of the molecular orbitals, as shown by Weltner and Van Zee.⁷ This explains why the odd-numbered anions are less stable and the odd-numbered neutral clusters are more stable. The effect is also seen in the geometries in Figs. 1 and 2. The bond lengths of even-numbered clusters shrink a little when the electron is attached, while the opposite happens for odd-numbered clusters.

D. C_nH clusters

There are no surprises in the ground-state geometries of the C_nH clusters (Fig. 4), which are all linear chains with minor Jahn–Teller distortions until $n=9$. The $C_{10}H$ is a cyclic structure with the H atom attached to one of the atoms in the ring. As expected, the H atom cannot be incorporated as a part of the ring because hydrogen has only one electron available for interaction and cannot be bonded with more than one atom. This is also the reason why the H atom is always at one end of the linear chains. Attempts to attach the hydrogen atom to other parts of the chains failed because, on geometry optimization, the hydrogen atom always moved to the end of the chain. Limited calculations on C_3H clusters yield³⁴ linear ground states with H attached to the end of the chain, as observed in our calculations.

The hydrogen atom may, however, be attached to any one of the atoms in a ring structure, and this may stabilize it

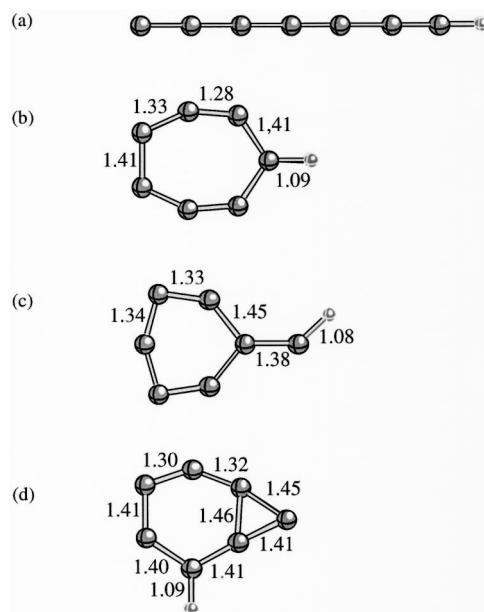


FIG. 5. Optimized geometries of C_7H clusters: (a) ground state; (b), (c), and (d) are low-lying isomers.

more than its linear isomer. This point was verified for the larger clusters and in each case (except $C_{10}H$) the linear structures were the ground states. As an example of the types of structures examined, we present four structures tested for C_7H with the H atom occupying different positions (Fig. 5). Here (a) is the ground-state cluster, which is linear, with the H atom attached to one end. Other structures are higher-energy isomers with geometries (b), (c), and (d), which are 0.91, 3.89, and 1.87 eV higher in total energy than the ground state.

The energies for the C_nH clusters are given in Table II. Note that the multiplicity is two for each cluster, as was also observed for the C_n^- . This can be explained by the fact that the addition of a H atom has the same effect as adding an extra electron. The C_nH and C_n^- clusters are therefore expected to behave similarly. As already mentioned, both have a spin-doublet configuration for all values of n under consideration. The binding energy of H with C_n should be expected to be similar to that of the AEAs of C_n clusters. These binding energies are plotted in Fig. 6 as a function of n . A comparison of Figs. 3 and 6 shows that the AEA plots of C_n and the binding energy of H with C_n clusters go through similar odd–even alternations with peaks at even- n values (except for the binding energy of H with C_n for $n=10$). A similar behavior is also shown by the ΔE of C_nH clusters with the peaks occurring for even values of n . The similarity of the effects of adding an electron and adding a hydrogen atom to C_n clusters is also reflected in the bond lengths. In both the cases the addition leads to a general shrinking of the bond lengths. For example, the bond in C_2 shrinks from 1.32 to 1.27 Å in C_2^- and to 1.24 Å in C_2H . We therefore conclude that similar changes occur in the electronic structures of the carbon clusters due to the addition of an electron or that of a H atom. Of course, this happens for even values of n , as these are the more stable of the C_n species. The effect is the opposite for odd- n clusters.

TABLE II. Results from C_nH and C_nH^- calculations. ΔE indicates the energy released when an extra carbon atom is added to a preexisting cluster. BE is the binding energy for a hydrogen atom to the corresponding C_n or C_n^- cluster.

n	C_nH				C_nH^-				AEA (eV)
	Multiplicity	E (hartree)	ΔE (eV)	BE (eV)	Multiplicity	E (hartree)	ΔE (eV)	BE (eV)	
1	2	-38.47434		3.65	3	-38.49067		3.72	0.44
2	2	-76.60598	7.86	5.01	1	-76.69517	9.84	4.63	2.43
3	2	-114.67707	6.21	3.46	3	-114.72656	5.13	3.23	1.35
4	2	-152.77346	6.90	4.87	1	-152.88079	8.47	4.53	2.92
5	2	-190.85148	6.40	3.74	3	-190.92468	5.47	3.36	1.99
6	2	-228.9416	6.73	4.77	1	-229.05907	7.93	4.43	3.20
7	2	-267.02125	6.45	3.95	3	-267.11053	5.68	3.55	2.43
8	2	-305.10844	6.65	4.73	1	-305.23314	7.61	4.41	3.39
9	2	-343.18867	6.46	4.08	3	-343.28987	5.82	3.70	2.75
10	2	-381.27847	6.72	2.78	1	-381.37703	6.65	4.24	2.68

E. C_nH^- clusters

Once again the calculated ground-state structures of C_nH^- (Fig. 7) are all linear up to $n=9$ and $C_{10}H^-$ is cyclic. Dreuw and Cederbaum³⁵ have theoretically examined many types of structures for C_7Cs^- and C_9Cs^- . Their results at the MP2 level show that there are many stable structures within 2 eV from the ground state, which, in each case, is linear with the Cs atom at the end of the chain. Their observation of “lightly embracing” structures was based upon the interaction of Cs^+ and C_n^- dianions. This is not a possible scenario for the interaction of H atoms, as it would not be able to give up its electron readily. Consequently, the usual, linear ground state is observed for C_nH and C_nH^- clusters.

The AEAs calculated from the energies of these clusters are given in Table II. The values of the AEAs, the binding energies of the H atom with C_n and C_n^- , and the ΔE of C_nH and C_nH^- are plotted in Fig. 6. All of these show the same type of odd–even alternation with peaks at even n . In each case the CH bond length is between 1.07 and 1.09 Å, which is the value commonly seen in literature. The experimental value³⁶ of the VEA for C_3H is 1.858 ± 0.023 eV, which is approximately 0.5 eV above the AEAs obtained from our

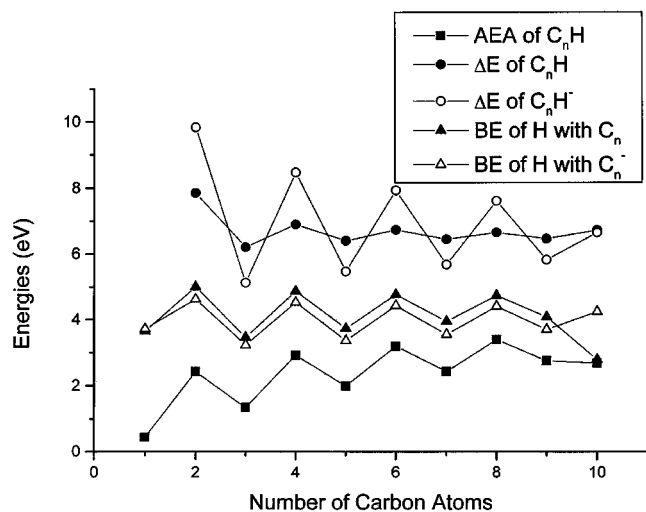


FIG. 6. Values of ΔE for C_nH (solid circles) and C_nH^- (open circles) clusters, binding energy of H with C_n (solid triangles) and C_n^- (open triangles), and adiabatic electron affinity of C_nH clusters.

calculations. This energy difference is similar to that observed between the experimental VEA and theoretical AEA values for C_n clusters (see Sec. II C and Table I). Experiments on the production and characterization of C_nH^- clusters show that the clusters are relatively more abundant for even n , which are relatively more stable (see Fig. 6). This will be further discussed in the subsequent section devoted to experimental results.

III. EXPERIMENTAL STUDY OF HYDROGENATED CARBON CLUSTERS

A. Production of C_nH^- clusters by gas-feed Cs sputtering

The gas-feed source of negative ions by cesium sputtering (GF-SNICS) is a well-established technique for generat-

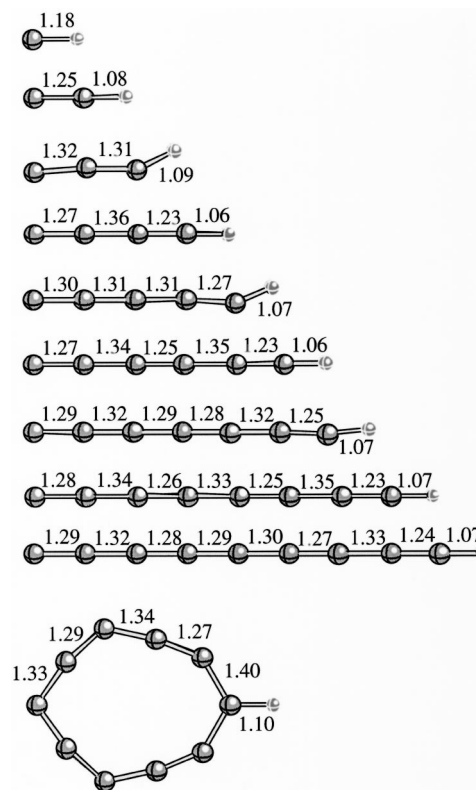
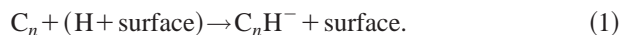


FIG. 7. Optimized ground-state geometries of C_nH^- ($n \leq 10$) clusters (bond lengths are in Å).

ing molecular anions and involves the spraying of an appropriate gas onto the cathode during sputtering. It is commonly employed in tandem accelerator facilities to produce molecular ions. We have used this technique to produce *mixed* cluster anions such as C_nN^- ($n \leq 10$) and have described it in detail in Ref. 10. A carbonaceous target such as graphite, amorphous C or C_{60} (in the form of a 4-mm-long and 4-mm-wide solid rod or pressed pellet) formed the sputter cathode. It was push fitted into an oxide-free, high-conductivity copper holder to ensure good thermal contact and sufficient cooling and, therefore, adequate Cs coverage of the sample of interest. The sputter cathode sample and sample mounting arrangement were modified to accommodate the gas spray system. The gas to be sprayed (H_2 , in this case) was introduced into the source through a 1-mm-bore stainless steel (SS) tube traversing through the center of a 10-mm-diam SS tube used for close loop-kerosene cooling and mounting of the cathode sample. A 1-mm-diam hole was drilled through the center of the SS stud and sample. The gas flow was controlled by a needle valve.

Sputtering of neutral as well as charged clusters occurs on bombarding the target surface by keV Cs^+ ions. The anionic species from the GF-SNICS source were extracted and focused into a beam by an Einzel lens. The anions were accelerated to ground potential from the negatively biased deck at -20 kV. A double-focusing 90° analyzing magnet with a mass-energy product of about $10 \text{ amu} \times \text{MeV}$ was used to select ions of particular m/q value. The slits were adjusted such that neighboring masses up to 300 amu could be well resolved. The anion yields were measured in a Faraday cup located near the image slits of the analyzing magnet with the help of a Keithley 485 picoammeter.

Our earlier study of C_nN^- suggests a surface origin of the gas-spray-induced negative ions.¹⁰ Similarly, we propose here that the C_nH^- ions are formed by a recombination reaction between neutral C_n clusters emerging from the surface and H atoms (formed by dissociative adsorption of H_2 preferentially at defect sites produced by Cs^+ bombardment) residing on the target surface which has a relatively low work function due to a fractional layer of Cs. The reaction is of the form



The surface acts as the third body to allow for conservation of momentum and energy in the reaction.

B. Yield of C_nH^- clusters

Figure 8 shows the characteristic growth of monohydrogen-substituted carbon cluster anions (C_nH^-) as a function of the pressure of H_2 gas, $p(H_2)$, introduced through the ejection crater in the graphite sample. The corresponding C_nH^- yield was measured as a function of $p(H_2)$ in the range of 1.0×10^{-7} – 2.0×10^{-5} Torr using an ion gauge controller near the ion source. The yield of C_nH^- initially rises with $p(H_2)$ for all n (growth curves for only some of the species are shown in Fig. 8), then saturates before falling steeply at higher pressure due to detachment and dissociation losses on colliding with residual gas molecules in the vicinity of the cathode. In order to minimize the loss of

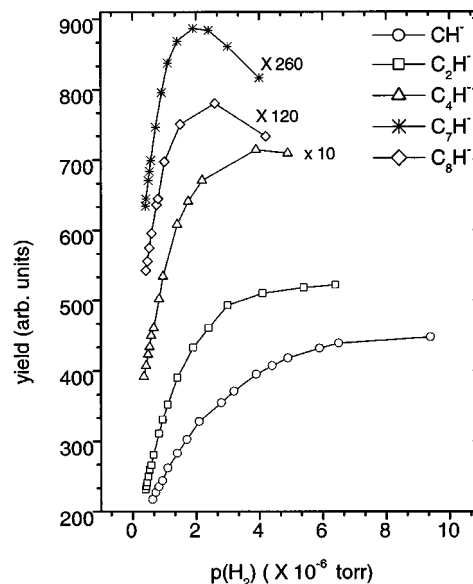


FIG. 8. Yields of the C_nH^- cluster anions generated by 5-keV Cs^+ ion sputtering of high-purity polycrystalline C as a function of hydrogen gas pressure. The growth curves are presented only for certain representative species.

sputter-ejected anions, our operating pressure $p(H_2)$ was kept less than 1.0×10^{-6} Torr. The Cs^+ ion bombardment energy was 2–5 keV. The typical intensity of the C_nH^- clusters was in the range of 0.05–90 nA under the usual operating parameters of the GF-SNICS.

C. Odd-even alternation in the cluster yield

Figure 9 shows the abundance distribution of the normalized intrinsic (without spraying H_2) carbon cluster anions C_n^- ($n \leq 10$) generated by sputtering of high-purity crystalline graphite by 5-keV Cs^+ ions. The base vacuum was 8.0×10^{-8} Torr. In general, the C_n^- yield declines with increasing cluster size. As expected from singly charged ion-induced sputtering, the size dependence of the yield exhibits

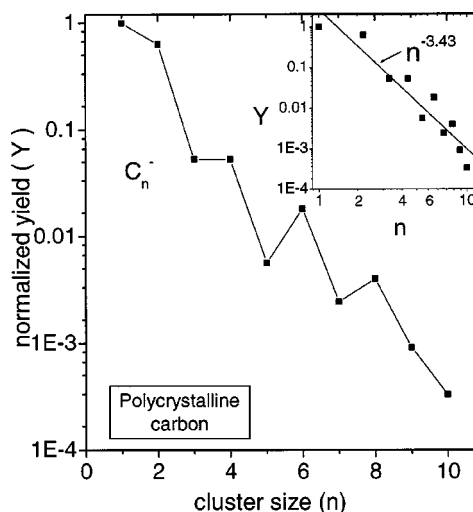


FIG. 9. Yield distribution of C_n^- cluster anions vs the cluster size n ($1 < n < 10$). These cluster anions are sputter-generated by 5-keV Cs^+ bombardment of polycrystalline C. Inset shows the log-log plot of the same data.

an odd–even oscillation.³⁷ UV photoelectron spectroscopy and other studies^{5,6,37} show that carbon clusters with $n < 10$ have linear-chain-like structures, while the larger ones form monocyclic rings.

Under similar operating conditions, the size dependence of the yields from amorphous carbon and fullerene (C_{60}) targets is quite similar to that from graphite, with an odd–even oscillation riding on a general decline with increasing n . The amorphous carbon target was cut from a high-purity carbon rod, whose amorphous nature was confirmed by x-ray diffraction. The fullerene target was prepared by pressing (at ~ 100 bars) 99.9% C_{60} powder into a pellet in the copper holder.

Figure 10 shows the normalized and background-subtracted yield distribution of the C_nH^- ($n \leq 10$) clusters Cs^+ sputtered from crystalline graphite in the presence of H_2 . The C_nH^- yield also declines with cluster number. Both odd- and even- n members are observed. The normalized yield of C_nH^- also exhibits an odd–even oscillations, with the even- n species being relatively more abundant. The C_nH^- ($n \leq 10$) clusters were also produced by sputtering of amorphous C and the fullerene targets in the presence of H_2 with $p(H_2) < 1.0 \times 10^{-6}$ Torr. The nature of the decline in yield with n is qualitatively similar for the different targets.

The normalized yields of sputter-ejected C_nH^- cluster anions from the three different polymorphs of carbon display an odd–even oscillation as a function of n : even- n clusters being relatively more abundant. Such an alternation can be qualitatively ascribed to the odd–even alternation in the adiabatic electron affinities of the C_nH^- clusters. Our density functional calculations of the ground-state geometries of C_nH^- show not only that the AEAs of the species with even n are larger than those with odd n , but also that the even- n cluster anions are relatively more stable. This is in contrast to the C_nN^- cluster anions where odd- n species are more abundant.¹⁰ This is attributed to the oscillatory values of the vertical electron detachment energy (VEDE) of C_nN^- clusters.³⁸ The strong correlation between C_nH^- yields and the computed electron affinity values clearly supports the notion that the abundance distribution of stable C_nH^- is largely determined by their electron affinities.

D. Power-law decline of the cluster yield

The insets in Figs. 10(a), 10(b), and 10(c) show the relative yield distributions of C_nH^- clusters sputtered from crystalline graphite, amorphous (am) C and fullerene, respectively, in the presence of H_2 . The inset in Fig. 9 shows the relative yield distribution for C_n^- clusters sputtered from crystalline graphite. The Cs^+ ion bombardment energy was 5 keV in all cases. The cluster size dependence of the relative yields measured far away from the sample surface can be approximated by a power law of the form

$$Y(n) \propto n^{-\delta}. \quad (2)$$

The least-squares-fit values of the exponent δ are shown in the insets to Figs. 9 and 10. Within experimental uncertainty, the values of δ for C_n^- cluster anions sputter ejected from crystalline and am-C (not shown) are virtually the same. The values of δ for C_nH^- cluster anions obtained from

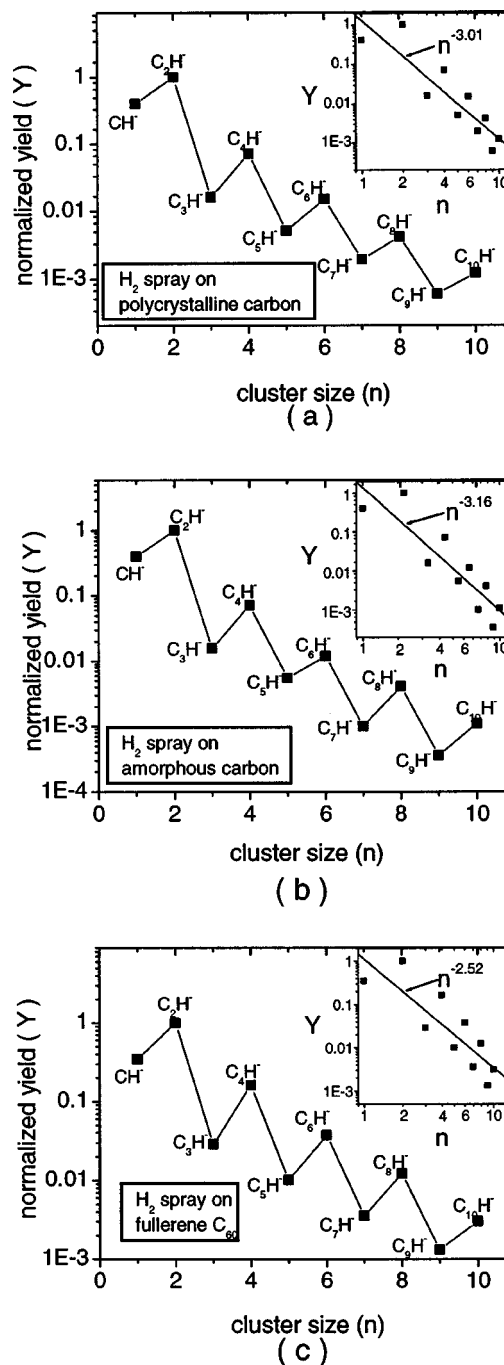


FIG. 10. Normalized and background subtracted yields of the cluster anions C_nH^- vs the cluster size n ($1 \leq n \leq 10$). The cluster anions were sputter generated by 5-keV Cs ion bombardment in the presence of H_2 gas from the surfaces of (a) polycrystalline carbon, (b) amorphous carbon, and (c) fullerene. Insets show log-log plots of the cluster anion (C_nH^-) yields vs cluster size n for the corresponding target material.

crystalline and am-C are also quite similar (Fig. 10). The close similarity in the relative yield distributions and power-law exponents related to the crystalline and am-C targets indicates that the ion-bombardment-induced structural evolution of the surface and subsurface atomic layers during the formation of sputtered clusters is quite similar. In other words, the energetics of the collision cascade does not appear to depend strongly on the crystalline structure of the two C-based targets.

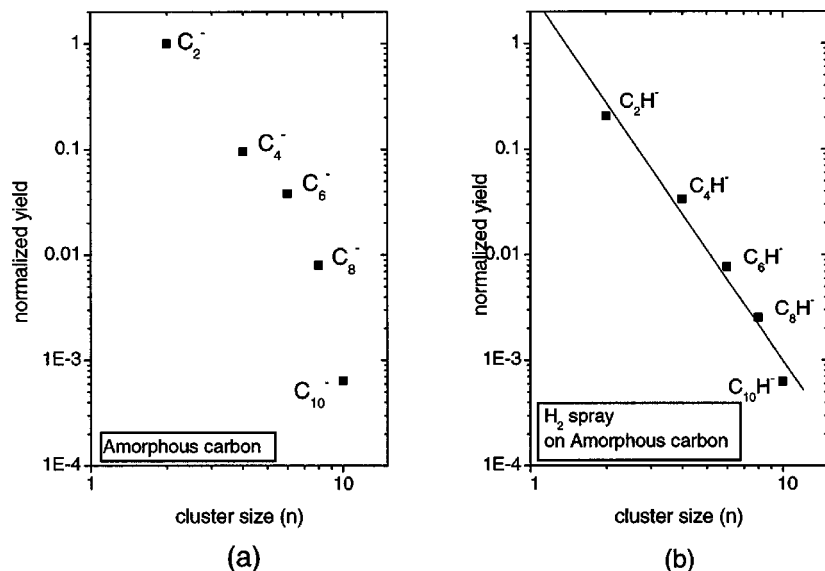


FIG. 11. (a) Cluster anion (C_n^-) yields vs cluster size n . (b) Cluster anion (C_nH^-) yields vs cluster size n . Both plots are from the amorphous carbon sample data. Only the even- n species are plotted in log-log scale.

We also point out that the fullerene-sputtered clusters differ from those of graphite and am-C in an important manner. The value of δ for C_nH^- clusters sputtered from the C_{60} surface is significantly higher than the polycrystalline and amorphous counterparts (Fig. 10) under similar operating conditions. This result is very similar to that in our earlier study on C_nN^- clusters¹⁰ and can probably be explained by a similar argument based on the densification of C_{60} that is known to occur on ion irradiation.³⁹ Thus, under Cs^+ irradiation, the sputtered surface of C_{60} may undergo structural changes associated with densification, resulting in a higher probability of dissociative and adsorption of H_2 at the surface. This, in turn, could lead to a greater yield of sputtered C_nH^- cluster anions than from graphite and am-C. Such an argument is supported by our observation that C_{60} -sputtered clusters yield a C_nH^-/C_n^- ratio that is higher by several factors as compared to graphite and am-C surfaces. Since this ratio (for the C_{60} target) increases rather rapidly with n , the power-law exponent (see Fig. 10) turns out to be unusually high (-2.52) compared to those of graphite (-3.01) or am-C (-3.16).

However, the fact that the yield distributions of the C_nH^- clusters sputtered from different crystallographic forms of carbon show a similar oscillatory behavior and follow a *single* power-law decline (in each case) indicates that the cluster formation does not depend *significantly* on the crystalline structure of the surface. This is in agreement with molecular dynamics simulations of cluster formation due to sputtering.⁴⁰

E. Chain to ring transformation

A majority of the experimental and theoretical work on small carbon clusters suggest that linear chains should be formed up to $n=9$, though it has not been possible to identify the actual isomeric structures experimentally. Even longer linear carbon chains ($n \geq 10$) can be produced by laser generation of the carbon plasma, but only when their ends are terminated by such groups as $-H$ or $-CN$.⁴¹

The abundance distribution of the sputter-ejected, pure carbon cluster anions C_n^- exhibits the expected odd-even oscillations with a sudden departure from its oscillatory pattern at $n=10$ (Fig. 9), which is normally attributed to a chain to ring transformation (CRT).^{5,6,37} The signature of this transformation is clearer from the log-log plot in Fig. 11(a), which shows a definite dip in the yield in the even- n family of C_n^- at $n=10$. In the case of the hydrogenated carbon cluster anions C_nH^- (Fig. 10), the yield does not appear to show any clear deviation from the oscillatory behavior at $n=10$. However, a close examination of the log-log plot in Fig. 11(b) shows that there *is* actually a deviation at $n=10$, though the magnitude of this deviation is much smaller than in the case of C_n^- . Such a deviation is observed in the data for graphite, am-C as well as fullerene, emphasizing its authenticity.

We interpret the above data to indicate that though the CRT *does* occur (as, indeed, expected from theoretical considerations), it appears to be suppressed to some extent. It is extremely interesting to point out in this context that our earlier study¹⁰ had established a *complete suppression* of the CRT in the nitrogenated carbon clusters C_nN^- . We believe that the sputtered C_{10} cluster is produced predominantly in the ringlike isomeric state. Now, the recombination probability of H with the ringlike isomer C_{10} at the ion-induced surface [see Eq. (1)] is likely to be lower than with the chain like one, as indicated by the fact that the computed bond strength of H with C_{10} is particularly low (see Table II). This results in a relatively lower yield of sputtered C_nH^- clusters. But the AEA of $C_{10}H^-$ ring is computed to be high enough, giving rise to higher emission probability (i.e., negative ionization efficiency) as $C_{10}H^-$ anions from the surface. As a result, we are likely to record relatively suppressed yield of ringlike $C_{10}H^-$ clusters formed during sputtering. Thus we infer that the sputter-ejected $C_{10}H^-$ cluster anion does undergo a CRT in agreement with our density functional calculations. However, the simultaneous existence of a fraction of chainlike $C_{10}H^-$ structures cannot be ruled out.

IV. SUMMARY

Theoretical calculations based on density functional methods were used to study the interaction of hydrogen with anionic as well as neutral carbon clusters. The geometry, stability, and electronic structure of C_nH^- clusters exhibit odd-even oscillations that are quite similar to the experimental abundance pattern for C_nH^- ($n \leq 10$) clusters produced by the hydrogen gas-feed Cs sputtering from different carbonaceous targets (graphite, amorphous-C and C_{60}). The yields of both even- and odd- n cluster anions were found to grow with an increasing H_2 pressure. The normalized yield of C_nH^- cluster anions sputter ejected from all three targets displays an oscillatory behavior as a function of n : clusters with even n being more abundant. This can be attributed to the oscillatory adiabatic electron affinities of these cluster anions. We have shown that the C_nH^- clusters produced from the C_{60} target exhibit certain different features in relation to graphite and amorphous carbon. The observed abundance distributions of the even members of C_n^- and C_nH^- indicate that, in conformity with our density functional calculations, monohydrogen substitution of the carbon clusters does allow the chain to ring transformation to occur at $n = 10$, but the transformation is partially suppressed. In contrast, mononitrogen substitution *totally* suppresses the chain to ring transformation at $n = 10$, in the case of C_nN^- clusters.

ACKNOWLEDGMENTS

Two of the authors (L.P.) and (B.K.R.) acknowledge partial support from a grant from the U.S. Department of Energy No. (DEFG02-96ER45579) to B.K.R. A.K.G. is grateful to Dr. S. Kailas for his encouragement and advice.

- ¹ *Novel Materials Design and Properties*, edited by B. K. Rao and S. N. Behera (Nova Science, New York, 1998); ed. *Science and Technology of Nanostructured Materials*, edited by B. K. Rao, S. M. Bose, M. P. Das, and S. N. Sahu (Nova Science, New York, 2001).
- ² P. Jena, S. N. Khanna, and B. K. Rao, in *Density Functional Theory of Molecules, Clusters, and Solids*, edited by D. E. Ellis (Kluwer Academic, Dordrecht, 1995), p. 123.
- ³ H. W. Kroto, J. R. Heath, S. C. O'Brien, R. F. Curl, and R. E. Smalley, *Nature* (London) **318**, 162 (1985); R. F. Curl and R. E. Smalley, *Science* **242**, 1917 (1988).
- ⁴ R. Saito, G. Dresselhaus, and M. S. Dresselhaus, *Physical Properties of Carbon Nanotubes* (Imperial College Press, London, 1998). See also references therein.
- ⁵ K. Raghavachari and J. S. Binkley, *J. Chem. Phys.* **87**, 2191 (1987). See also references mentioned therein.
- ⁶ S. Yang, K. J. Taylor, M. J. Craycraft, J. Conceicao, C. L. Pettiette, O. Cheshnovsky, and R. E. Smalley, *Chem. Phys. Lett.* **144**, 431 (1988); G. von Helden, P. R. Kemper, N. G. Gotts, and M. T. Bowers, *Science* **259**, 1300 (1993); D. W. Arnold, S. E. Bradforth, T. N. Kitsopoulos, and D. M. Neumark, *J. Chem. Phys.* **95**, 8753 (1991).
- ⁷ W. Weltner, Jr. and R. J. Van Zee, *Chem. Rev.* **89**, 1713 (1989).
- ⁸ G. L. Gutsev, S. N. Khanna, and P. Jena, *Phys. Rev. B* **62**, 1604 (2000); S. N. Khanna and P. Jena, *Chem. Phys. Lett.* **336**, 467 (2001).

- ⁹ D. K. Bohme and S. Wlodek, *Int. J. Mass Spectrom. Ion Processes* **102**, 133 (1990); Q. L. Zhang, S. C. O'Brien, J. R. Heath, Y. Liu, R. F. Curl, H. W. Kroto, and R. E. Smalley, *J. Phys. Chem.* **90**, 525 (1986); S. W. McElvany, W. R. Creasy, and A. O'Keefe, *J. Chem. Phys.* **85**, 632 (1986).
- ¹⁰ A. K. Gupta and P. Ayyub, *Eur. Phys. J. D* **17**, 221 (2001).
- ¹¹ H. W. Kroto, J. R. Heath, S. C. O'Brien, R. F. Curl, and R. E. Smalley, *Astrophys. J.* **314**, 352 (1988); R. P. Hallett, K. G. McKay, S. P. Balm, A. W. Allaf, H. W. Kroto, and A. J. Stace, *Z. Phys. D: At., Mol. Clusters* **34**, 65 (1995).
- ¹² T. Schlatholter, M. W. Newman, T. R. Niedermayr, G. A. Machicoane, J. W. McDonald, T. Schenkel, R. Hoekstra, and A. V. Hamza, *Eur. Phys. J. D* **12**, 323 (2000).
- ¹³ M. Leleyter, *Z. Phys. D: At., Mol. Clusters* **12**, 381 (1989).
- ¹⁴ M. Wagner and K. Wien, *Nucl. Instrum. Methods Phys. Res. B* **82**, 362 (1993).
- ¹⁵ R. Huang, C. Wang, Z. Liu, L. Zheng, F. Qi, L. Sheng, S. Yu, and Y. Zhang, *Z. Phys. D: At., Mol. Clusters* **33**, 49 (1995).
- ¹⁶ M. J. Frisch, G. W. Trucks, H. B. Schlegel *et al.*, GAUSSIAN 98, revision A.7, Gaussian, Inc., Pittsburgh, 1998. Also see references therein.
- ¹⁷ C. Lee, W. Yang, and R. G. Parr, *Phys. Rev. B* **37**, 785 (1988).
- ¹⁸ A. D. Becke, *J. Chem. Phys.* **98**, 5648 (1993).
- ¹⁹ J. A. Nichols and J. Simons, *J. Chem. Phys.* **86**, 6972 (1987).
- ²⁰ D. C. Harris and M. D. Bertolucci, *Symmetry and Spectroscopy, an Introduction to Vibrational and Electronic Spectroscopy* (Dover, New York, 1989).
- ²¹ B. K. Nash, B. K. Rao, and P. Jena, *J. Chem. Phys.* **105**, 11 020 (1996). See also references therein.
- ²² K. Raghavachari, *Chem. Phys. Lett.* **171**, 249 (1990).
- ²³ K. W. Hinkle, J. J. Keady, and P. F. Bernath, *Science* **241**, 1319 (1988).
- ²⁴ L. Adamowicz, *Chem. Phys.* **156**, 387 (1990); *J. Chem. Phys.* **94**, 1241 (1991); J. P. Ritchie, H. F. King, and W. S. Young, *ibid.* **85**, 5175 (1986); J. D. Watts, J. Cernusak, and R. J. Bartlett, *Chem. Phys. Lett.* **178**, 259 (1991).
- ²⁵ L. Adamowicz and J. Kurtz, *Chem. Phys. Lett.* **162**, 342 (1989).
- ²⁶ K. Raghavachari, R. A. Whiteside, and J. A. Pople, *J. Chem. Phys.* **85**, 6623 (1986); V. Parasuk and J. Almlöf, *ibid.* **91**, 1137 (1989).
- ²⁷ Z. Slanina, J. Kurtz, and L. Adamowicz, *Chem. Phys. Lett.* **196**, 208 (1992).
- ²⁸ Z. Slanina, S. L. Lee, J. P. Francois, J. Kurtz, and L. Adamowicz, *Chem. Phys. Lett.* **223**, 397 (1994).
- ²⁹ Z. Slanina, S. L. Lee, J. P. Francois, J. Kurtz, L. Adamowicz, and M. Smigel, *Mol. Phys.* **81**, 1489 (1994).
- ³⁰ B. K. Rao and P. Jena, *Phys. Rev. B* **32**, 2058 (1985).
- ³¹ L. Adamowicz, *Chem. Phys. Lett.* **182**, 45 (1991); *Chem. Phys.* **156**, 387 (1991).
- ³² A. K. Ray and B. K. Rao, *Z. Phys. D: At., Mol. Clusters* **33**, 197 (1995).
- ³³ N. G. Gotts, G. von Helden, and M. T. Bowers, *Int. J. Mass Spectrom. Ion Processes* **149/150**, 217 (1995); G. von Helden, W. E. Palke, and M. T. Bowers, *Chem. Phys. Lett.* **212**, 247 (1993).
- ³⁴ S. Green, *Astrophys. J.* **240**, 962 (1980); D. L. Cooper, *ibid.* **265**, 808 (1983).
- ³⁵ A. Dreuw and L. S. Cederbaum, *J. Chem. Phys.* **111**, 1467 (1999).
- ³⁶ J. M. Oakes and G. B. Ellison, *Tetrahedron* **42**, 6263 (1986).
- ³⁷ G. Gnaser and H. Oechsner, *Nucl. Instrum. Methods Phys. Res. B* **82**, 518 (1993).
- ³⁸ C. Wang, R. Huang, Z. Liu, and L. Zheng, *Chem. Phys. Lett.* **237**, 463 (1995).
- ³⁹ D. Fink *et al.*, *Fullerene Sci. Technol.* **6**, 911 (1998).
- ⁴⁰ G. Betz and W. Husinsky, *Nucl. Instrum. Methods Phys. Res. B* **102**, 281 (1995); A. Wucher and B. J. Garrison, *J. Chem. Phys.* **105**, 5999 (1996); J. W. Hartman, M. H. Shapiro, and T. A. Tombrello, *Nucl. Instrum. Methods Phys. Res. B* **132**, 406 (1997).
- ⁴¹ J. R. Heath, Q. Zhang, S. C. O'Brien, R. F. Curl, H. W. Kroto, and R. E. Smalley, *J. Am. Chem. Soc.* **109**, 359 (1987).